Two-Stage Indoor Positioning using Deep Learning and RF Fingerprinting in WiFi Networks

Rafael Saraiva Campos e Lisandro Lovisolo,

***Abstract*— This work addresses the problem of radio frequency machine learning-based indoor multifloor positioning, by proposing a two-stage localization scheme. On the first stage, a majority voting committee of Deep Neural Networks (DNN) identifies the floor where the mobile station (MS) is most likely located. On the second stage RF fingerprinting, also known as Database Correlation Method (DCM), provides an estimate of the MS location within the selected floor. In DCM, target RF fingerprints - measured by the MS to be localized - are compared with georeferenced RF fingerprints, previously stored in a correlation database (CDB). The performance of the proposed solution is experimentally evaluated using 40800 target fingerprints and a CDB with 816 reference fingerprints, containing Received Signal Strength (RSS) values of 115 WiFi 802.11b/g networks spanning 3 floors. The proposed two-stage scheme achieved floor identification accuracies ranging from 91 to 97%, and mean planar positioning errors from 1.4 down to 0.4 meters.**

***Keywords*— multifloor positioning, deep learning, RF fingerprinting, correlation function**

I. Introduction

There is a growing number of Mobile Stations (MSs) equipped with built-in Global Positioning System (GPS) receivers. In open areas, GPS yields high precision location estimates, but is usually unavailable in indoor environments. In this scenario, Received Signal Strength (RSS) based location techniques are used both in cellular and Wireless Fidelity (WiFi) networks [1]. In cellular mobile telephony, indoor positioning might rely on the reception of signals from indoor micro or even picocells, or from outdoor cells with strong indoor reception [2]. However, the increasingly denser deployment and availability of WiFi access points (APs), coupled with the fact that most mobile devices today are WiFi enabled, makes the use of WiFi signals a preferable choice for indoor positioning, in comparison to cellular mobile telephony signals [3].

When implementing or using a location-based system (LBS) for indoor positioning, one may not be troubled by small planar errors. For example, suppose that one is in a garage or mall, if the LBS estimates or indicates that an object or MS is within three or five meters from its actual location, this error may be acceptable. However, if the LBS reports that one is on the wrong floor this may not be acceptable at all, mostly due to the fact that buildings are built in such a way that it is much easier to move within the same floor than among floors. Thereby, the most critical issue in WiFi indoor positioning is floor identification in multistorey buildings. This work addresses this issue by proposing a two-stage positioning scheme, as depicted in Fig 1: on the first stage, a majority voting committee of Deep Neural Networks (DNN) identifies the floor; then, on the second stage RF fingerprinting, also known as Database Correlation Method (DCM), provides an estimate of the MS location within that floor. DCM techniques provide a position fix by comparing a target RF fingerprint (TFing) – a set of RF parameters measured by the MS to be located – with a set of georeferenced and previously collected RF fingerprints, referred to as reference RF fingerprints (RFings) and stored in a Correlation Database (CDB) [4].

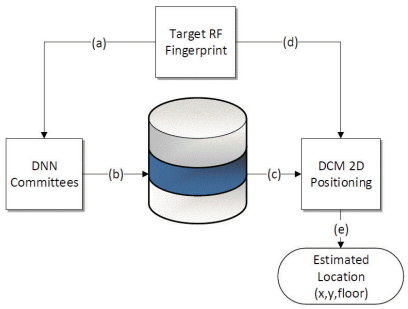

Fig. 1. Diagram of the proposed two-stage positioning scheme.

The remainder of this work is organized as follows: Section II describes the measurement campaign use to build the data sets used to validate the proposal; Section III details the first stage of the localization scheme, i.e., floor identification using a committee of DNNs; Section IV presents the second stage, i.e., the DCM technique used to provide a 2D position fix within the selected floor; Section V brings the experimental results; Section VI compares the results with the ones of other RF-based multifloor positioning engines. Finally, Section VII brings a brief conclusion.

II. Data Sets of WiFi RSS Measurements

A. Measurement Campaign

In this work, we use a subset of the database generated during a WiFi RSS measurement campaign carried out in the 13 floors of Reitor Joao Lyra Filho Pavilion at the Rio de Janeiro State University (UERJ) [5]. The software used to collect the WiFi scans was *NetStumbler* version 0.4 running in a Toshiba A75-S211 laptop with an Atheros AR5005GS built-in 802.11b/g adapter. *NetStumbler* forces the WiFi adapter to carry out a passive scan of 802.11 networks, i.e., without sending probe requests. For each detected AP, the MAC (Medium Access Control) address, SSID (Service Set Identifier), carrier

Rafael Saraiva Campos (Engenharia de Computação, CEFET/RJ, Petrópolis) e Lisandro Lovisolo (DETEl, UERJ, Rio de Janeiro). Emails: rafael.campos@cefet-rj.br e lisandro@uerj.br

number, noise level and signal-to-noise ratio were stored. The laptop was placed over a wheeled table, and at each of the 924 measurement points the WiFi adapter collected between 180 and 240 WiFi scans, at a rate of one per second. The measurement points are not distributed uniformly throughout the floors, with floors 4, 5, and 6 comprising 816 out of the 924 points, with approximately 270 points per floor. As a result, we selected only the WiFi RSS samples collected at the 4th, 5th, and 6th floors. Fig. 2 shows a perspective spatial view of the selected measurement points positions in the UERJ main building.

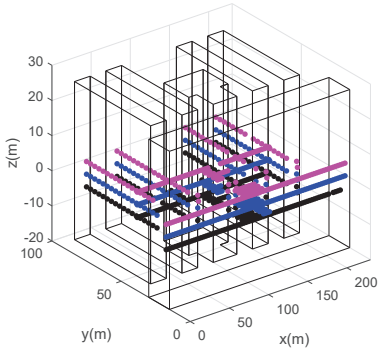

Fig. 2. Selected measurement points at UERJ main building, located on the 4th (black), 5th (blue), and 6th (magenta) floors.

B. RFings

Each measurement point is identified by a unique RFing containing the mean RSS values (in the logarithmic scale, ranging from -120 to -30 dBm) of each WiFi network detected at that particular location. The first 50 WiFi scans at each location are not included in this calculation, being reserved to test the proposed two-stage location engine. A total of $N = 115$ WiFi networks were detected at $N_p = 816$ different positions. The RFing of the kth point is defined by

$$\mathbf{f}_k = \left[\overline{\text{RSS}}_{1,k} \ldots \overline{\text{RSS}}_{N,k} \right] \tag{1}$$

where $\overline{\text{RSS}}_{i,k}$ denotes the average RSS from AP i at point k, for $i = 1, \ldots, N$ and $k = 1, \ldots, N_p$. This average is calculated by

$$\overline{\text{RSS}}_{i,k} = \frac{1}{H_{i,k}} \sum_{h=1}^{H_{i,k}} \text{RSS}_{i,k,h} \tag{2}$$

where $H_{i,k}$ denotes the number of occurrences of network i at point k, and $\text{RSS}_{i,k,h}$ indicates the measured RSS of network i, during the hth WiFi scan collected at point k. Note that, as the first 50 scans are reserved to be used in the test set, one has $50 < h \leq 240$, as 240 is the maximum number of scans at any given point. If a WiFi network is detected in less than 10% of the WiFi scans at a given point, its mean RSS value is not included in the RFing.

C. CDB

Each RFing is associated with a 3-tuple of geographic coordinates (x, y, z), where x and y are continuous variables representing the planar coordinates of the measurement locations within each floor, and z is a discrete variable which indicates the floor number. So, the kth CDB entry is given by the 4-uple $(\mathbf{f}_k, x_k, y_k, z_k)$, with $k = 1, \ldots, N_p$. The CDB is used to train the Deep-Learning (DL) classifiers.

D. TFings

Each of the first 50 WiFi scans at each measurement point corresponds to a TFing. RFings and TFings have the same structure, so a TFing is defined by the N-component vector

$$\mathbf{f} = [\text{RSS}_1 \ldots \text{RSS}_N] \tag{3}$$

The set of TFings is used to test the DL classifiers.

III. First Stage: Floor Identification using Committees of DNNs

In multifloor indoor positioning, it is very important to correctly identify the floor where the MS is located, before estimating the MS 2D position within that floor. It is particularly relevant for certain types of positioning applications, like emergency call location [6][7] and applications designed to help blind people locate the floor they are in [8]. A common strategy to design classifiers aiming at *a priori* defined outputs (e.g., the floor number) is the use of supervised clustering systems. In this work, we employ ensemble learning with bagging (bootstrap aggregating) [9]. In this technique, M subsets of the training data are randomly formed by sampling with replacement, and each subset trains a different supervised classifier. The output of the M classifiers is then combined using majority voting. Outputs of majority voting committees are expected to have a lower variance than outputs of single binary classifiers, smoothing the stochastic component inherent to DNNs training and providing a more reliable and stable classification [10].

A. Topology

Autoencoders (AEs), convolutional neural networks (CNNs), deep belief networks (DBNs), and recurrent neural networks (RNNs) are the most commonly used DL architectures [11]. In this work, we use sparse AEs: each of the $M = 31$ classifiers in the majority voting committee is obtained by stacking two sparse autoencoders and a softmax layer. The size of the committee (i.e., the value of M) was empirically defined. Fig. 3 shows a schematic representation of an AE, with its two stages: the encoder and the decoder. The encoder can learn a more compact representation of the input data (if there are fewer neurons in the hidden layer than in the input layer), so one of its main uses is for dimensionality reduction [12]. The decoder attempts to recover the original data from the encoder output.

Each DNN in the majority voting committee is built by stacking two AEs. Following, a softmax layer is added. Fig. 4 depicts the DNNs topology. For the first AE, one has $m =$

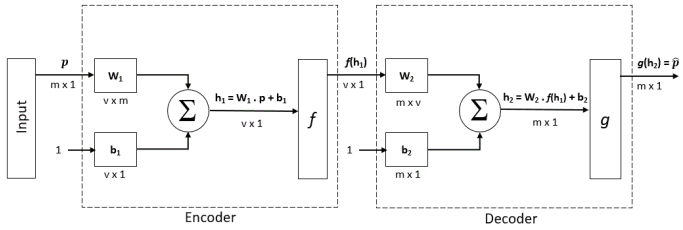

Fig. 3. Autoencoder topology, where m is the number of input nodes (i.e., the number of components of the input vector $\mathbf{p}$); v is the number of neurons in the hidden layer; $\mathbf{W}_1$ and $\mathbf{W}_2$ are the synaptic weights matrices of the encoder and decoder; $\mathbf{b}_1$ and $\mathbf{b}_2$ are the bias vectors of the encoder and decoder; f and g are the activation functions of the neurons in the hidden and output layers, respectively. The decoder yields an approximation $\hat{\mathbf{p}}$ of input vector $\mathbf{p}$.

$N = 115$ (the number of WiFi networks detected during the data collecting phase) and $v = 70$. For the second AE, one has $m = 70$ (as it receives as inputs the outputs of the first encoder) and $v = 35$. The activation functions f and g of the hidden and output layers of the AEs are the sigmoid and linear functions, i.e., $f(h) = 1/(1 + \exp(h))$ and $g(h) = h$, respectively. The final layer has 3 neurons (one for each class, i.e., floor) with softmax transfer functions. Thus, the output of the ith neuron is given by $s_i = \frac{\exp(h_i)}{\sum_{i=1}^{3} \exp(h_i)}$, where h_i is the aggregate input of the ith neuron. The output class is indicated by the neuron which yields the highest output value in the softmax layer.

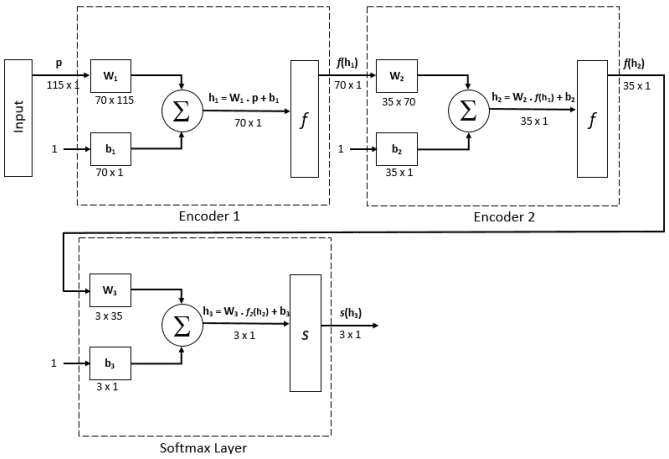

Fig. 4. Topology of the DNN, where S indicates a softmax layer.

B. Training

1) AEs: the first AE is trained using the RFings in the CDB. The second AE is trained using the outputs of the first encoder. The performance function used for batch training both AEs is the mean squared error (MSE) with L2-norm and sparsity regularization

$$E = \frac{1}{N_p} \sum_{k=1}^{N_p} \sum_{i=1}^{N} \left(f_{ik} - \hat{f}_{ik} \right)^2 + \lambda \Omega + \beta \Psi \qquad (4)$$

where $N_p = 816$ is the number of RFings in the CDB, $N = 115$ is the number WiFi networks per RFing, Ω is the L2-norm regularization term, Ψ is the sparsity regularization term, $\lambda = 1$ and $\beta = 0.001$, $\mathbf{F} = [f_{ik}]_{i=1,\ldots,N;k=1,\ldots,N_p}$ is the training set, and $\hat{\mathbf{F}} = [\hat{f}_{ik}]_{i=1,\ldots,N;k=1,\ldots,N_p}$ is the output set.

The L2-norm regularization term Ω penalizes solutions with larger DNN weights, which would make the AE unstable [9]. This term is given by

$$\Omega = \sum_{j=1}^{N} \sum_{i=1}^{v} (w_{ij}^{(1)})^2 + \sum_{j=1}^{v} \sum_{i=1}^{N} (w_{ij}^{(2)})^2 \qquad (5)$$

where $\mathbf{W}_1 = [w_{ij}^{(1)}]_{i=1,\ldots,v;j=1,\ldots,N}$ and $\mathbf{W}_2 = [w_{ij}^{(2)}]_{i=1,\ldots,N;j=1,\ldots,v}$ are the encoder and decoder weight matrices, respectively.

The sparsity regularization term Ψ is larger when the average activation value (output) of the neurons in the hidden layer (averaged over the entire training set in batch training) are distant in value from the desired average value ρ. The term Ψ is given by the Kullback-Leibler divergence [13], i.e.,

$$\Psi = \sum_{i=1}^{v} KL\left(\rho || \hat{\rho}_i\right) = \sum_{i=1}^{v} \left[\rho \log\left(\frac{\rho}{\hat{\rho}_i}\right) + (1-\rho) \log\left(\frac{1-\rho}{1-\hat{\rho}_i}\right) \right] \qquad (6)$$

where $\hat{\rho}_i$ is the average activation value of the ith neuron in the hidden layer, and $\rho = 0.05$ (empirically defined). Low average activation values mean that the neurons fire just to a few samples in the training set. So, adding a sparsity regularization term to the cost function helps the encoder to learn a representation where each neuron responds to just a small subset of training examples, specializing to some features that are present only in that subset.

2) Softmax Layer: the softmax layer is trained using the output of the second encoder; the cost function used to train it is the cross-entropy, defined by $E = -\mathbf{T} \log(\mathbf{Y})$, where $\mathbf{T}$ is the target matrix and $\mathbf{Y}$ is the matrix containing the outputs produced by the softmax layer.

3) DNN: the network formed by stacking the aforementioned layers (as in Fig. 4) is trained using scaled conjugate gradient descent learning method and cross-entropy cost function (defined by the softmax layer). Early stopping was not used (as no part of the training set was reserved for validation), so the stop criterion is the number of epochs (1000).

IV. Second Stage: DCM 2D Positioning

In order to estimate the MS location, it is necessary to compare the TFing with the RFings in the CDB. The first stage of the proposed localization scheme selects a floor, so the correlation space within the CDB is restricted to the points within the selected floor. Let set $\mathcal{D}$ be this reduced search space within the CDB. The higher the similarity or correlation between the TFing and an RFing in $\mathcal{D}$, the higher the probability that the MS is located at the RFing's coordinates. This similarity is assessed by means of an evaluation or correlation function. In this work, two such correlation functions are considered.

A. First Correlation Function

The MS is assumed to be located at the point whose RFing has the highest correlation or similarity with the TFing. Let $\mathbf{f}$

be the TFing measured by the MS to be localized, as defined by Eq. (3), and $\mathbf{f}_k$ be the RFing associated with the kth point, given by Eq. (1). The first similarity measure is defined as inverse of the Euclidean distance between these fingerprints in the N-dimensional RSS space, i.e.

$$f_{1,k} = \left[(\mathbf{f} - \mathbf{f}_k) (\mathbf{f} - \mathbf{f}_k)^{\mathrm{T}} \right]^{-1} \tag{7}$$

B. Second Correlation Function

Another approach would use a regularization term that penalizes candidate solutions (i.e., RFings) with more mismatches in relation to WiFi networks with RSS values above -120 dBm in the TFing. In this case, the identity of the detected networks would have a higher impact in the correlation than solely their RSS values. This might mitigate the detrimental effect of RSS variations (e.g., due to multipath fading) and of cross-device conditions (i.e., trying to locate a MS of a different model than the one used to build the CDB).

Let $\mathcal{T}$ and $\mathcal{R}_k$ be the set of WiFi networks with RSS above -120 dBm listed in the TFing and the RFing associated with the kth point, respectively, for $k \in \mathcal{D}$. The set $\mathcal{C}_k$ contains the network IDs occurring both in $\mathcal{T}$ and $\mathcal{R}_k$, i.e., $\mathcal{C}_k = \mathcal{T} \cap \mathcal{R}_k$. Let $\mathcal{S}_T$ and $\mathcal{S}_{R,k}$ be the sets containing the RSS values – in the TFing and the kth RFing, respectively – of the networks listed in $\mathcal{C}_k$. The value of the correlation between the TFing and the kth RFing now is defined as

$$f_{2,k} = \left[\alpha N \left| \#\mathcal{T} - \#\mathcal{C}_k \right| + \sum_{i=1}^{\#\mathcal{C}_k} \left| s_{T,i} - s_{R,k,i} \right| \right]^{-1} \tag{8}$$

where $\#\mathcal{T}$ is the cardinality of $\mathcal{T}$, $\#\mathcal{C}_k$ is the cardinality of $\mathcal{C}_k$, α is the dynamic range of RSS, $s_{T,i}$ and $s_{R,k,i}$ are the ith elements of $\mathcal{S}_T$ and $\mathcal{S}_{R,k}$, respectively. The first term in Eq. (8) is the penalty due to the absence in $\mathcal{R}_k$ of networks that are in $\mathcal{T}$. The second term calculates the absolute cumulative difference between the elements of $\mathcal{S}_T$ and $\mathcal{S}_{R,k}$. If all networks listed in $\mathcal{T}$ are also in $\mathcal{R}_k$, then $\mathcal{C}_k \equiv \mathcal{R}_k \equiv \mathcal{T}$, so $\#\mathcal{C}_k = \#\mathcal{T}$, and the first term in Eq. (8) is null. In the worst case scenario, where $\mathcal{C}_i = \oslash$, the first term in Eq. (8) reaches its maximum value and the second term is null. Regarding the penalty term, consider the pth and qth points. For each network listed in $\mathcal{T}$ and not in $\mathcal{R}_p$ or $\mathcal{R}_q$, a αN value is added to $f_{2,p}$ or $f_{2,q}$, respectively. As α is equal to the maximum variation of RSS, the first term in Eq. (8) ensures that if $\#\mathcal{C}_p > \#\mathcal{C}_q$, then $f_{2,p} > f_{2,q}$, regardless of the second term value.

V. Experimental Results

As previously indicated, the first 50 WiFi scans per point are reserved to test the localization system, so one has $50 \times 816 = 40800$ test samples. The performance of the localization system is evaluated in terms of floor identification accuracy (first stage) and DCM 2D positioning error (second stage). For that, different window lengths are considered. The window length (in seconds) indicates the quantity of subsequent RSS measurements (collected at a rate of 1 Hz) that are averaged to compose the TFing. Larger windows (10 and 25 sec) are better suited to model the behavior of stationary or slow moving MS. Shorter windows (1 and 5 sec) better represent the dynamics of MS carried by someone walking.

Fig. 5 shows the floor identification accuracy yielded by the first stage (DNN committee) of the positioning scheme. The achieved accuracies range from 91% (using a single WiFi scan) up to 97% (using 25 subsequent WiFi scans).

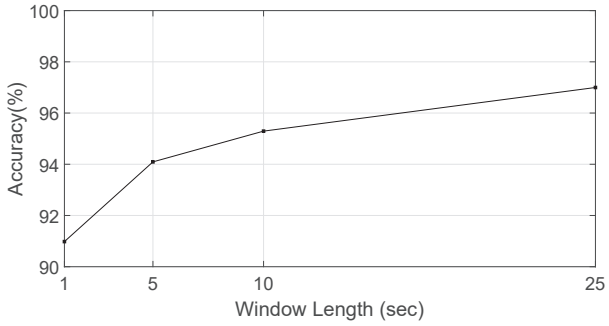

Fig. 5. Floor identification accuracy per window length.

Fig. 6 brings the cumulative distribution function (CDF) of the 2D positioning error achieved by DCM using the second correlation function, as defined by Eq. (8). As expected, the precision increases with the window length. However, one notes that, even for a window length of 1 sec (just one WiFi scan composing the TFing), the positioning error is lower than 6.9 meters for 95% of the test samples. One might note some discontinuities in the CDF plots. Those derive from the test points distribution being discrete, forming a planar grid with 3 meters separation between adjacent points. In fact, the largest "jump" occurs precisely at 3 meters. Smaller discontinuities occur at multiples of that distance.

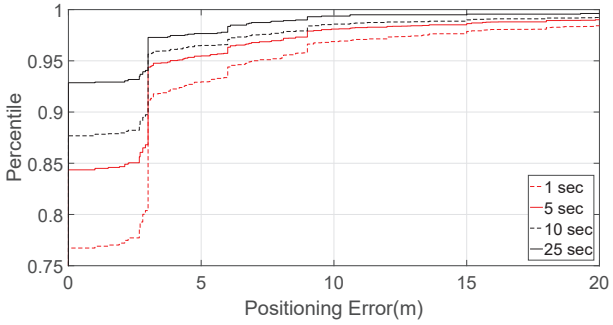

Fig. 6. CDF of DCM 2D positioning error per window length using correlation function f_2. This graph considers only the error associated with TFings whose floor was correctly identified by the DNN committee in the first stage.

Fig. 7 shows the mean and the 95th percentile of the DCM 2D positioning error achieved using correlation functions f_1 and f_2 for different window lengths. Notably, f_2 reduces the 95th percentile, in comparison to f_1, by 1.3 meter with a window length of 1 sec, and by 2 meters, with a window length of 5 sec. For larger window lengths, the improvement is negligible. The same applies to the mean error, for all window lengths.

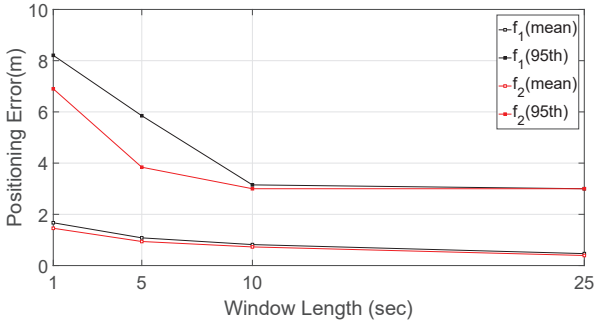

Fig. 7. Mean value and 95th percentile of DCM positioning error per window length. This graph considers only the error associated with TFings whose floor was correctly identified by the DNN committee in the first stage.

VI. Comparison with Other Published Results

In [5] the authors used a three-stage localization engine: first, non-supervised clustering using a Kohonen layer to select a multifloor subset of RFings within the CDB, followed by supervised classification using multilayer perceptrons (MLP) to identify the floor within the cluster provided by the first step, and then DCM positioning to estimate the MS location within the reduced search space provided by the previous two stages. The proposal evaluated using a data set with 46200 TFings (WiFi scans, each containing RSS values of up to 136 WiFi networks) collected in 924 points spread through 12 floors. They achieved floor identification accuracies ranging from 91% to 97%, and average 2D positioning error between 4.5 to 1.7 meters, for window lengths from 1 to 25 seconds, respectively. As already mentioned in Section II, our present work uses a subset of that same database, selecting only the points within the 4th, 5th and 6th floors, which comprise 88% of all points, i.e., the number of samples collected at the other 9 floors is too small (approximately only 12 per floor) to properly train the DNN classifiers. Besides that, this asymmetry might comprise the reliability of the floor identification accuracy.

In [14] the authors developed an RSS-based multilateration positioning system called SaskEPS (Saskatchewan Enhanced Positioning System). It achieved 100% floor identification accuracy, in a testbed comprising two buildings with three floors each; 25 test points were selected per floor per building, totalizing 150 test locations. The system requires careful calibration of the propagation models used to estimate the distance between the target MS and each of the APs listed in the WiFi scan, and that the coordinates of all APs are very accurately known.

In [15] the authors used a Bayesian Graphic Model (BGM) to obtain position fixes. The authors reported an average planar positioning error of 2.3 meters in a testbed with 600 samples gathered in 30 test points distributed in two floors. The floor identification accuracy was not informed.

In [16] the authors used DCM with KNN - in what was called Nearest Floor Algorithm - for floor identification only, achieving a 86% accuracy using a data set comprising 150 points distributed among 3 floors.

VII. Conclusion

This work proposes the use of a two-stage indoor positioning scheme for localization in multistorey buildings. The first stage employs DNN committees to identify the floor. The second stage performs DCM 2D positioning using the reduced search space provided by the first stage, i.e., the selected floor. Two different correlation functions were considered for the DCM phase. The proposed two-stage scheme achieved floor identification accuracies ranging from 91 to 97%, and mean planar positioning errors from 1.4 down to 0.4 meters, for window lengths from 1 up to 25 seconds, respectively.

Referências

[1] R. Bill et al. “Indoor and outdoor positioning in mobile environments - a review and some investigations on WLAN positioning”, *Geographic Information Sciences*, v. 10, n. 2, 2004.

[2] H. Liu et al., “Survey of Wireless Indoor Positioning Techniques and Systems”,*IEEE Transactions on Systems, Man, and Cybernetics, Part C: Applications and Reviews*, v. 37, n. 6, pp. 1067–1080, 2007.

[3] C. Laoudias et al., “The Airplace indoor positioning platform for Android smartphones”, *2012 IEEE 13th International Conference on Mobile Data Management (MDM)*, pp. 312–315, 2012.

[4] R. S. Campos, L. Lovisolo, and M. L. de Campos, “Search space reduction in DCM positioning using unsupervised clustering”, *Proceedings of IEEE 10th Workshop on Positioning Navigation and Communication (WPNC)*, pp. 1–6, Dresden, Germany, March 2013.

[5] R. S. Campos, L. Lovisolo and M. L. R. de Campos, “Wi-Fi Multifloor Indoor Positioning considering Architectural Aspects and Controlled Computational Complexity”, Expert Systems with Applications, v. 41, n. 14, pp. 6211–6223, October, 2014.

[6] A. Varshavsky et al, “The SkyLoc Floor Localization System”, *Proceedings of the Fifth Annual IEEE International Conference on Pervasive Computing and Communications (PerCom’07)*, pp. 125–134, White Plains, USA, March, 2007.

[7] N. Moayeri, J. Mapar, S. Tompkins, and K. Pahlavan, “Emerging opportunities for localization and tracking”, *IEEE Wireless Communications*, vol.18, n.2, pp. 8–9, 2011.

[8] Y. Bai et al, “Helping the blind to find the floor of destination in multistory buildings using a barometer”, *35th Annual International Conference of the IEEE Engineering in Medicine and Biology Society (EMBC)*, pp. 4738–4741, Jul 2013.

[9] S. Marsland, “Machine Learning: An Algorithmic Perspective”, CRC Press, New York, 2008.

[10] F. Leisch and K. Hornik, “ARC-LH: A new adaptive resampling algorithm for improving ANN classifiers”, Advances in Neural Information Processing Systems, pp. 522–528, 1997.

[11] J. E. Ball, D. T. Anderson, and C. S. Chan, “Comprehensive survey of deep learning in remote sensing: theories, tools, and challenges for the community”, Journal of Applied Remote Sensing, vol.11, n.4, Sep 2017.

[12] G. Hinton and R. Salakhutdinov, “Reducing the dimensionality of data with neural networks”, Science, vol. 313, no. 5786, pp.504–507, 2006.

[13] S. Kullback, R. A. Leibler, “On Information and Sufficiency”, The Annals of Mathematical Statistics, vol. 22, no. 1, pp 79–86, 1951.

[14] S. Bell, W. Jung, and V. Krishnakumar, “WiFi-based Enhanced Positioning Systems: Accuracy Through Mapping, Calibration, and Classification”, *Proceedings of the 2nd ACM SIGSPATIAL International Workshop on Indoor Spatial Awareness*, pp. 3–9, San Jose, California, 2010.

[15] A. Al-Ahmadi et al., “Multi-floor indoor positioning system using Bayesian graphical models”, *Progress in Electromagnetics Research B*, v. 25, pp. 241–259, 2010

[16] F. Alsehly, T. Arslan, and Z. Sevak, “Indoor positioning with floor determination in multi story buildings”, *2011 International Conference on Indoor Positioning and Indoor Navigation (IPIN)*, pp. 1–7, Sep 2011.